



Claire Murphy  
November 2017

This thesis submitted in accordance with the requirements of the University of Adelaide for an Honours Degree in Geology

# A reconstruction of Late Pleistocene to Holocene palaeoenvironmental change at Basin Lake, Fraser Island

**A RECONSTRUCTION OF LATE PLEISTOCENE TO HOLOCENE  
PALAEOENVIRONMENTAL CHANGE AT BASIN LAKE, FRASER ISLAND**

**FRASER ISLAND PALAEORECORD**

**ABSTRACT**

Fraser Island lake sediments may record valuable information about past environmental changes, which in turn may provide key insights into the mechanisms driving this variability. This information is vital if we are to determine how the Fraser Island environment has reacted to climate changes in the past, and by extension, how it may react to similar conditions in the future. In this study, the geochemical composition of sediments from Basin Lake, Fraser Island, were characterised using a combination of organic and moisture content analyses, micro-XRF analysis, traditional XRF analysis, X-ray diffraction, particle size analysis and radiocarbon dating. The Basin Lake sediments contain a mixture of locally derived sand and far travelled dust, in proportions that have varied through time. Changing environmental conditions resulted in the deposition of four distinct sediment units within the lake. The new data presented here indicates that regional scale aridity was a dominant influence on sediment deposition on Fraser Island at or before 49 thousand years before present, resulting in a high percentage of distally sourced sediment in Basin Lake. During the Last Glacial Maximum, extreme local aridity resulted in increased contribution from locally-derived sediment before a return to wetter conditions during the early Holocene. The Late Holocene sediments preserve evidence for greater climate variability, alternating between arid and wet environments.

**KEYWORDS**

Dust, palaeoenvironments, lake sediments, scanning XRF, X-Ray diffraction, grain size analysis



## TABLE OF CONTENTS

A reconstruction of Late Pleistocene to Holocene palaeoenvironmental change at Basin Lake, Fraser Island .....	i
Abstract.....	i
Keywords.....	i
List of Figures and Tables .....	3
Introduction .....	4
Geological Setting/Background.....	7
Methods .....	10
Results .....	12
Geochronology .....	12
Loss on ignition .....	14
Magnetic susceptibility.....	14
iTrax high resolution XRF.....	14
Discrete XRF.....	17
X-Ray Diffraction (XRD).....	18
Particle size distribution .....	19
Discussion.....	19
Definitions of local sand and far travelled dust.....	19
PCA and how elements relate to dust (regional) or sand (local) inputs. ....	21
Comparison of discrete and continuous XRF samples.....	21
Discontinuity of the record.....	22
Segment A, 404-262 cm, (>49.7 ka) .....	22
Hiatus I (~28kyr) .....	24
Segment B, 262-235 cm (LGM).....	24
Segment C, 235-68 cm, 11-8 ka .....	25
Hiatus II.....	26
Segment D 0-68 cm, 0-5 ka.....	26
Conclusions .....	28
Acknowledgments .....	29
References .....	30
Appendix A: Extended Methods .....	33
Core splitting .....	33
Loss on ignition .....	33
ITRAX.....	33

Particle size analysis .....	34
XRD .....	34
XRF .....	34
Appendix b: Core Photographs .....	35

## LIST OF FIGURES AND TABLES

Figure 1 Location map of Fraser Island including elevation.....	7
Figure 2 A cross section of the dune systems on Fraser Island. Image sourced from Marshall et al. 2015. ....	9
Figure 3 Bayesian age-depth model for Basin Lake, Fraser Island, 0-5 m (corrected depth).....	13
Figure 4 The organic matter, magnetic susceptibility, particle size distribution and itrax data from Basin Lake, Fraser Island.....	15
Figure 5 Principal components analysis of the 12 recorded elements, separated by the segments of the core. ....	16
Figure 6 Si in cps against sand as considered by grain size, and Si/Ti against sand as considered by grain size .....	20
Table 1 Results of the radiocarbon dates produced at ANSTO. Displayed is the measured age, the error and the corrected age for each sample, along with their lab ID and the material that was dated. The depth of the material includes corrections for compactions and is at one depth rather than a range as was the inputs for the Bayesian Age model package. ....	12
Table 2 Elemental abundances of discrete XRF samples.....	17
Table 3. Results of the XRD, including the depth of the sample and the segment of the core that the samples fall into. The samples with a '*' next to their depths were also analysed for discrete XRF. ....	18

## INTRODUCTION

Palaeoclimate studies provide vital information for future climate model simulations (Robinson & Dowsett, 2012) as our knowledge of current climate change is informed by our understanding of past climate change and variability (Nieto-Moreno et al., 2014). Robust palaeoclimate records enable a reduction in the uncertainty of climate predictions (Robinson & Dowsett, 2012). Global scale changes may have highly variable effects on the environment on regional scales, as a function of the resilience of the local environment. Hence, it is important that a wide range of environments are studied, so that it can be predicted how the same changes to global climate may effect local environments differently.

Lakes on Fraser Island may provide high-resolution records of environmental change, providing valuable records of long term change (Hembrow & Taffs, 2012) which provide a tool for future environmental predictions to be made. Valuable environmental records have been derived from proxies including diatoms, pollen, and charcoal at lakes including Lake Allom, Lake McKenzie, and Hidden Lake (Donders, Wagner, & Visscher, 2006; Hembrow & Taffs, 2012; Longmore, Heijnis, Partridge, Kershaw, & Iriondo, 1999; Woltering et al., 2014). These studies have produced records for environmental change on Fraser Island, temporally and spatially, with documented changes varying between study sites. However, these studies have all produced records focused on palaeo biomarkers, with no previous studies producing a geochemical record of lake sediments on Fraser Island. This leaves a large knowledge gap, with no information about the chemical and mineralogical composition of the sediments which are accumulating in the lakes on Fraser Island.

Inferred dry and windy conditions during the last glacial maximum (LGM), 18-24 thousand years before present (ka) (Mix et al. 2001), probably resulted in lake drying conditions on Fraser Island, causing hiatuses in sedimentation (Atahan et al., 2013; Donders et al., 2006; Hembrow & Taffs, 2012; Thomas, Nott, Murray, & Price, 2007; Woltering et al., 2014). Studies on different lakes have shown these hiatuses to occur across different time periods. Some studies have attributed the hiatuses to a dry lake (e.g. Donders et al., 2006), whilst others have attributed it to an intermittently or seasonally dry lake (Atahan et al., 2013; Hembrow & Taffs, 2012; Woltering et al., 2014). In contrast, on nearby NSI, the LGM is characterised by the highest rates of sedimentation, due to the higher flux of inorganic sediments (McGowan, Petherick, & Kamber, 2008). The LGM on Fraser Island was characterised by a drier climate than was experienced in previous glacials (Longmore et al., 1999).

Continuous sedimentary records are highly valuable, as they can provide continuous records of past climates. Chronological analyses do not always support continuous sedimentation, however the timing, duration and causes of hiatuses in deposition can provide information about extreme climatic events. Several lake sediment records on Fraser Island exhibit loosely correlating hiatuses, indicative of dry lakes. The cause of the variations in timing of events recorded in lakes on Fraser Island is not yet understood.

The effects of the El Niño Southern Oscillation (ENSO) are propagated globally and is defined by adiabatic warming and cooling of the Pacific Ocean (Frauen & Dommenges, 2010) and leads to oscillations between El Niño and La Niña (Martin-Rey, Rodriguez-Bonseca, & Polo, 2015). Increasing intensity of ENSO in the late Holocene may have resulted in oscillations from arid to wet climates, with a consequent increase



in aeolian sediment transport and accumulation. For transportation of inorganic sediment to occur, there must be an event supporting sediment resupply, immediately followed by transporting conditions (Marx, McGowan, & Kamber, 2009). Wetter climates associated with La Nina conditions allows the supply of the material, and the drier climates associated with El Niño allows transportation. Consistent with studies on the nearby NSI, it may be expected that sediment was derived from a more distal source in the Pleistocene, changing to a more local source during the Holocene (McGowan et al., 2008; Petherick, McGowan, Kamber, Bauer, & Lancaster, 2009). At 3.9 ka, on North Stradbroke Island, a change in the ratio of local to regional sediment sources suggests that only 13% of the sediment was regionally sourced, compared to approximately 50% at 20.1 ka (Petherick et al., 2009). During the late Holocene (2.7-1.8 ka), even drier conditions on Fraser Island (Donders et al., 2006) are evidenced through aquatic plants and charcoal records.

Due to arid conditions inferred on Fraser Island during the LGM, we may expect to see hiatuses in sedimentation, representing lake drying events as a result of the aridity associated with the Last Glacial Maximum. This is, indeed, what has been observed in previous work (Donders et al., 2006; Longmore, 1998).

The aim of this paper is to address the lack of geochemical records on Fraser Island and hence produce a record of past environmental variability locally (on Fraser Island) and continentally, by analyzing preserved environmental indicators from a sediment core from Basin Lake, Fraser Island (Figure 1). A range of analyses including particle size distribution, iTrax, XRF, XRD, and organic matter content were used to infer the type and provenance of lithic materials in the sediments, in order to address

local and regional climate variability. The timing of deposition of these features was determined through radiocarbon dating.

## GEOLOGICAL SETTING/BACKGROUND

Fraser Island is located off the coast of Queensland (Figure 1) and is the largest sand island in the world, at 120 km long. Fraser Island achieved status as a world heritage site in 1992. The International Union for Conservation of Nature (IUCN) application for status included the unique features of Fraser Island, as it is the only place in the world where rainforests grow on sand dunes, and hosts a large number of the worlds freshwater perched sand dune lakes (WCMC/IUCN 1992).

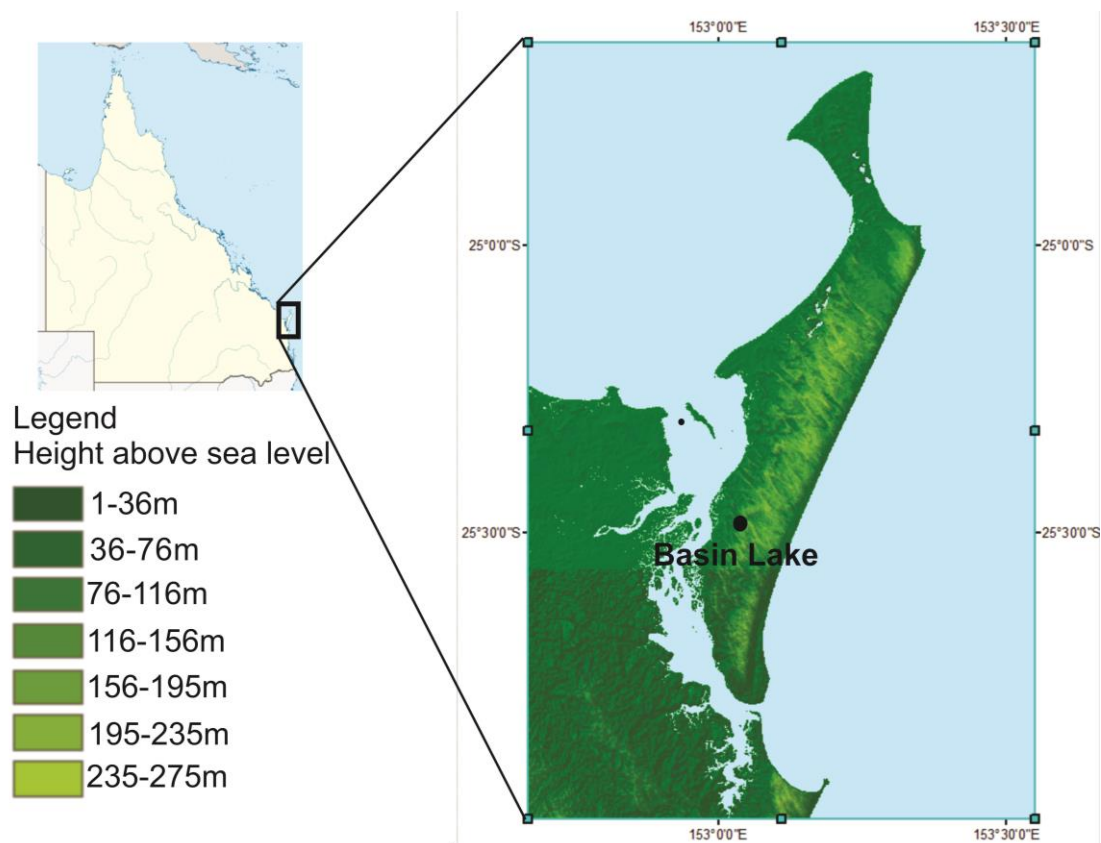


**Figure 1. Location map of Fraser Island including elevation**

Fraser Island falls within the Maryborough Basin, which is a rift basin composed of Late Triassic to Early Tertiary aged rocks. Along the margins of the basin, intrusive

rocks from the Mesozoic were emplaced (Marshall, Fontaine, Kilgour, & Lewis, 2015) and often lies beneath the sedimentary rock, with occasional outcrops. The elevation of the Maryborough Basin is quite low, with the exception of Fraser Island, due to the height of overlying parabolic sand dunes (Marshall et al., 2015).

Few geochronological constraints have existed for sediments preserved on Fraser Island. However, inferences about dune emplacement can be made from information from the nearby Cooloola sand mass and NSI (Lees, 2006). Dune emplacement at these locations has been dated as occurring during glacial periods at 730 ka, 460 ka, 395-280 ka, 215-295 ka and 170-130 ka (Lees, 2006; Tekan-Kella et al., 1990). Sediment was transported alongshore and landward from the continental shelf and is responsible for deposition of the Fraser Island sand (Gontz et al., 2015; Lees, 2006). The sand dunes on Fraser Island are a part of the Australian Dune fields, which developed when sea levels fell, fluvial deltas were exposed, and experienced deflation (Lees, 2006). This occurred in 8 discrete stages recognised through thermoluminescence dating (Lees, 2006), resulting in the placement of the sand dunes on Fraser Island.

The western side of the island is dominated by coastal plains, Pleistocene aged dunes occur across the centre of the island, and Holocene aged dunes along the eastern coast (Figure 2). The island also features numerous lakes, that fall into one of two categories; groundwater lakes and perched lakes (Figure 2), (Marshall et al., 2015).

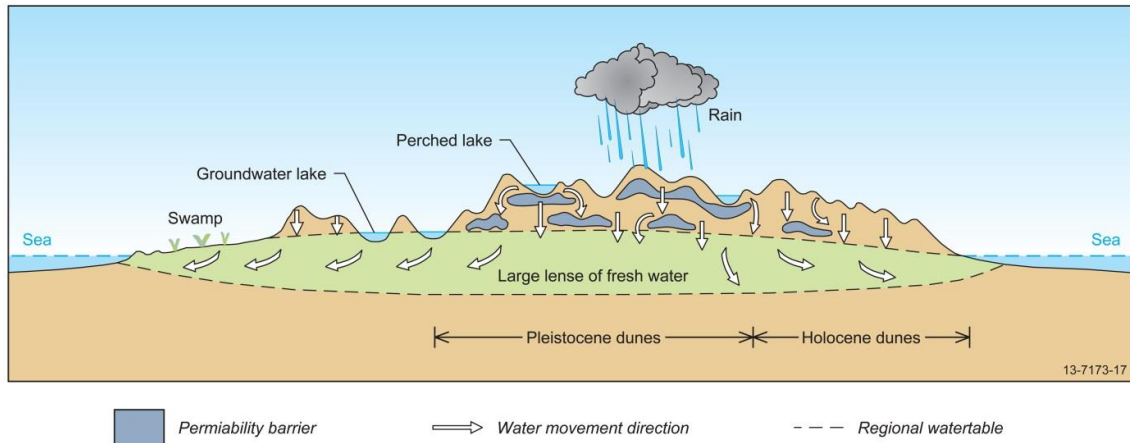


**Figure 2. A cross section of the dune systems on Fraser Island. Image sourced from Marshall et al. 2015.**

Fraser Island hosts a large number of the worlds perched sand dune lakes, which are lakes that are isolated from groundwater systems. Perched lakes occur when sediment become organically cemented (Gontz et al., 2015). The lake water inputs are entirely from rainfall, and the outputs are from evaporation or out-seepage. Thus, any inputs of sediment, nutrients, or organic material results in accumulation, and these perched lakes may act as ‘rain gauges’ (Donders et al., 2006).

In the Late Pleistocene, from 36.9-18.3 ka, global glaciation resulted in conditions that were drier, cooler and windier than present (Atahan et al., 2013). From 30-22 ka temperatures on Fraser Island dropped by approximately 1°C (Woltering et al., 2014) coincident with the pre glaciation and relatively cool and dry conditions from the Late Pleistocene (Donders et al., 2006).

From 13.3-12 ka the highest temperatures on Fraser Island occurred (of approximately 21.5°C, 1.1°C warmer than todays Mean Annual Air Temperature (MAAT)), (Woltering et al., 2014). At the onset of the Holocene, 12-8 ka, temperatures were close to modern (Woltering et al., 2014). From 8-5ka temperatures were slightly higher than present (about 0.9°C warmer than todays MAAT), and from 5 ka to present

temperatures were similar to temperatures today, perhaps slightly cooler (Woltering et al., 2014).

## **METHODS**

In November 2016, a 5 m core was collected from Basin Lake, Fraser Island, using a Bolivia corer. The core was collected in one meter intervals and refrigerated at 4°C. The upper 4 m was analysed, and the bottom metre stored for future study. As a result of the nature of the coring process, compactions of the sediment core may occur. As these compactions are likely different between each of the 5 drives, to make sure that these compactions do not affect the age model they must be compensated for by correcting the compaction error. This was done by taking the length of core, which was pushed into the sediment, dividing it by the length of core tube that was recovered, and multiplying each increment by this factor to get the true depth of the sediment. Throughout the rest of this paper depths will be referred to as uncorrected depths, unless mentioned otherwise.

The core was sub-sampled every centimetre for moisture content and organic matter content. The sub-samples were dried for 12 hours at 105°C before being ignited in a muffle furnace at 550°C for 4 hours to determine the moisture content and organic matter content of the samples, respectively.

The core was also sub-sampled at 4 cm intervals for particle size analysis. 10 g of sediment was subsampled and digested with Hydrogen Peroxide (H<sub>2</sub>O<sub>2</sub>) (50%) while being heated to 80°C. Each sample was centrifuged and the supernatant discarded. The samples were stored in 1 mL of dispersant, sodium hexametaphosphate ((NaPO<sub>3</sub>)<sub>6</sub>), (0.5 M), before being analysed for particle size distribution on a Mastersizer 2000, at the Australian Nuclear Science and Technology Organisation (ANSTO).

The core was taken to ANSTO for micro XRF (iTrax) analysis at 1 mm resolution. iTrax was conducted using a chromium-helium target x-ray tube. The XRF conditions were 30 kV, 55 mA and the x-radiograph conditions were 50 kV 30 mA with a 10 second count time per increment. This method of chemical analysis was chosen due to the large amount of elemental information that can be obtained rapidly; the non-destructive nature of the analysis; and the extremely small increments that the data can be collected on.

Due to the semi-quantitative nature of iTrax, sub-samples were selected for XRF and XRD analysis at approximately 20 cm intervals. These sub-samples were also digested with H<sub>2</sub>O<sub>2</sub> in the manner explained above, and oven dried at 70°C.

Twenty samples selected for XRD analysis were analysed at the University of Adelaide. Of these, 5 samples were selected for XRF analysis at Bureau Veritas. These samples were ground until 85% of grains passed through a 75 µm mesh.

Terrestrial material was sieved out of the sediment at points where the loss on ignition data showed extreme changes, and sent to ANSTO for radiocarbon dating. A Bayesian age model was developed in R using the Bacon program (Blaauw & Christen, 2011).

## RESULTS

### Geochronology

**Table 1. Results of the radiocarbon dates produced at ANSTO. Displayed is the measured age, the error and the corrected age for each sample, along with their lab ID and the material that was dated. The depth of the material includes corrections for compactions and is at one depth rather than a range as was the inputs for the Bayesian Age model package.**

Depth (cm)	Lab ID	Material dated	Age (years BP)	Error (years)	Corrected age (years BP)
19.3	D1, 11-12 cm	Woody fragment	1,105	35	967
43.9	D1, 25-26 cm	Stick fragment	2,455	35	2,431
87.7	D1, 50-51 cm	Woody fragment	3,745	30	4,049
120.6	D2, 19-20 cm	Leaf fragments	8,030	60	8,871
172.6	D2, 70-71 cm	Stick	8,840	50	9,777
280.4	D3, 76-77 cm	Woody fragment	9,455	50	11,097
308.0	D4, 5-6 cm	Woody fragment	18,520	150	19,685
321.2	D4, 15-16 cm	Woody fragments	46,010	630	49,733
491.0	D5, 67-68 cm	Woody fragments	46,593	700	50,157

Nine radiocarbon dates were analysed at ANSTO (Table 1), and an age depth model was produced using Bayesian age-depth modelling. After several iterations of the Bacon model, it was determined that the best output occurred with the conditions of hiatuses set at 112, 290 and 315 cm (corrected depth). Sedimentation rates were determined as 40 yr/cm from 0-68 cm (uncorrected depth) (present to 5.5 ka), 20 yr/cm from 68-241 cm (8.5-11 ka), 300 yr/cm from 241-262 cm (11-23 ka), and 2.5 yr/cm from 262-400 cm (49 ka to the base of the core). The dates produced indicate increasing age down the depth of the core (Figure 3), as expected, without any indication of influx periods of older material relative to the sedimentation trends.

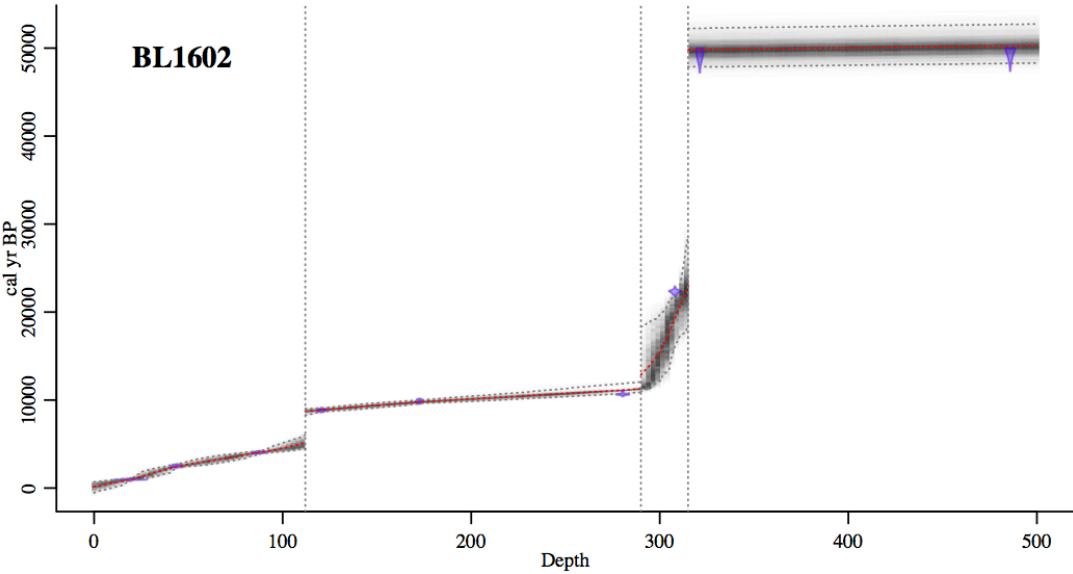


Figure 3. Bayesian age-depth model for Basin Lake, Fraser Island, 0-5 m (corrected depth).



## **Loss on ignition**

Throughout the record, organic matter was the dominant component of the dry sediment, with values of organic matter commonly above 90% of the dry sediment. Minimum values of the organic matter component are approximately 15%, when inorganic matter is at a high of approximately 85%, which occurs at 21 cm.

The moisture content of the sediment reflects that of the organic matter, showing that the moisture of the sediment is greatly held in the organic matter (Figure 4). At the most recent part of the core, the inorganic content is approximately 20% and the moisture content is approximately 90%.

## **Magnetic susceptibility**

For the entire length of the core, the magnetic susceptibility was found to be negative (Figure 4). Most commonly, the magnetic susceptibility varies between -1 CGS and -2 CGS. When there is a slight peak in inorganic content at approximately 380 cm, the magnetic susceptibility experiences a negative excursion. A similar negative excursion corresponds to a peak in inorganic matter at approximately 150 cm. However, not every peak in inorganic content has a corresponding negative magnetic susceptibility excursion. Magnetic susceptibility approaches zero at approximately 250 cm and 60 cm. This coincides with peaks in Fe and Ti from the iTrax data.

## **iTrax high resolution XRF**

High resolution XRF analysis taken on millimetre scale was analysed as individual elements. The following elements were detected by the iTrax scanner. When viewing

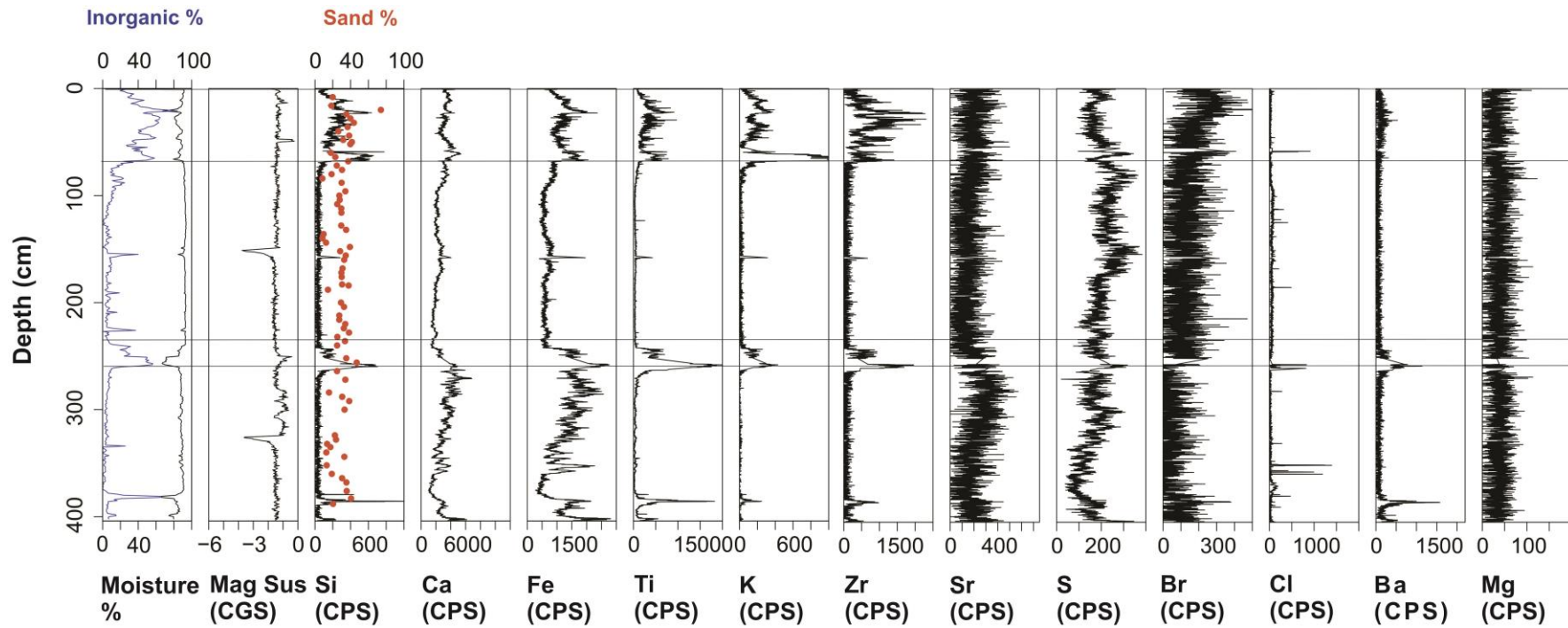


Figure 4. The organic matter, magnetic susceptibility, particle size distribution and itrax data from Basin Lake, Fraser Island.

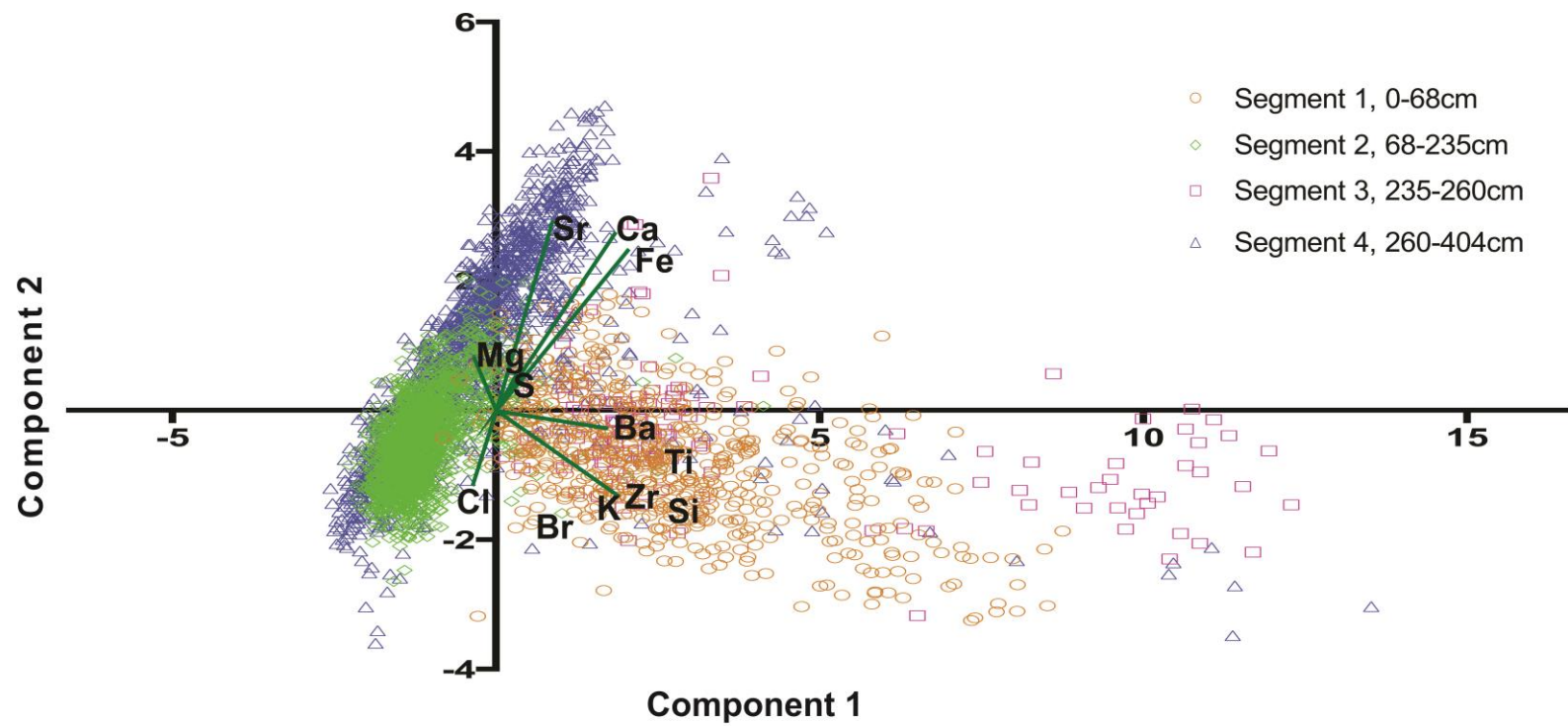


Figure 5. Principal components analysis of the 12 recorded elements, separated by the segments of the core.

the raw data, silicon appears in the greatest abundances without noise from 0-67 cm (5-0 ka), before decreasing to a low value of around 100 cps, which continues to about 230 cm, with a peak of about 300 cps at about 150 cm. From 230 cm, the silicon levels increase to about 700 cps at approximately 255 cm. This value decreases to the low levels of about 100 cps until about 380 cm where the highest peak of silicon appears of approximately 1000 cps.

Principle components analysis (PCA) was completed on the elements from the iTrax data. The results show that Ti, Zr and K are correlated with Si; and that Sr, Ca and Fe and not correlated with these elements (Table 3). In order to further the discrimination between the elements, a second PCA was undertaken using only the four correlated elements, Ti, Zr, K and Si. The resulting PCA still records a great deal of variation occurring, with Ti and Zr highly correlated, but display less correlation with Si and K.

### Discrete XRF

Discrete XRF was undertaken in order to confirm the iTrax elemental data (Table 2). The highest elemental abundances in the discrete samples were extremely high in Si in comparison to all other elements (Table 2). Many elements (including Ca, Ti, Fe) present in high abundances in the iTrax elemental data are present in very small abundances in the discrete XRF samples.

**Table 2. Elemental abundances of discrete XRF samples.**

Depth	Fe %	Si %	Al %	Mg %	P %	S %	K %	Ca %	Ti %
10-11cm	0.32	36.37	0.49	0.00	0.03	0.01	0.09	0.01	0.06
27-28cm	0.31	42.58	0.13	0.01	0.01	0.01	0.02	0.00	0.08
46-47cm	0.21	40.39	0.20	0.01	0.01	0.01	0.06	0.01	0.05
66-67cm	0.19	37.48	0.41	0.01	0.01	0.01	0.14	0.04	0.03
383-384cm	0.1	40.36	0.23	0.01	0.01	0.00	0.03	0.00	0.08

## X-Ray Diffraction (XRD)

XRD analysis indicated that the dominant mineral was quartz (Table 2). The XRD results provided support for the elemental iTrax data. Illite is present in most samples, but not from depths of 270-390 cm. Illite contains K, as well as Mg, Al, Fe, Si, H and O. If potassium is considered as the limiting factor, it occurs in the iTrax data with the least abundance from 260cm- 380cm, which matches the discrete XRD measurements showing lack of illite. Microcline also contains potassium as a limiting element, and is only present in samples also containing illite, and where the iTrax data shows higher values of K. The presence of albite also corresponds with the iTrax data. Albite typically contains Na, Al, Si and O, however the sodium may be replaced with Ca. The discrete XRD samples which contain albite also occur when there are peaks in calcium in the iTrax data. This is consistent with anorthite, which is a similar chemical composition to albite. Whilst quartz is present in all of the samples, the most defined XRD peaks occur when the iTrax data reflect high levels of silicon.

**Table 3. Results of the XRD, including the depth of the sample and the segment of the core that the samples fall into. The samples with a '\*' next to their depths were also analysed for discrete XRF.**

		Quartz	Kaolinite	Illite	Albite	Microcline	Biotite	Anorthite
Segment 4	10-11cm *	✓	✓	✓				
	27-28cm *	✓						
	46-47cm *	✓	✓	✓				
	66-67cm *	✓	✓	✓	✓	✓		
	89-90cm	✓	✓	✓				
Segment 3	110-111cm	✓	✓	✓			✓	
	130-131cm	✓	✓	✓				
	156-157cm	✓	✓	✓				
	174-175cm	✓	✓	✓				
	191-192cm	✓	✓	✓	✓			
Segment 2,	209-210cm	✓	✓	✓				
	226-227cm	✓	✓	✓				
	247-248cm	✓	✓	✓	✓			
	271-272cm	✓	✓		✓			✓
	291-292cm	✓	✓					
Segment 1	313-314cm	✓	✓	✓				
	335-336cm	✓	✓					
	357-358cm	✓	✓					
	383-384cm *	✓	✓					
	395-396cm	✓	✓	✓				

## **Particle size distribution**

Particle size distribution of the inorganic fraction was conducted on samples taken every 4 cm, on approximately 70% of the inorganic rich samples. Clay (grain sizes <0.004 mm) levels in the sediment were extremely low, the average clay fraction was 0.29%. The minimum silt (grain sizes 0.004 to 0.062 mm) fraction was 25.7%, which occurred at 20 cm. The maximum silt fraction was 91.6%, which occurred at 140 cm. The average silt fraction was 70.6%. The minimum sand (grain sizes 0.062 to 2 mm) fraction was 8.4%, which occurred at 84 cm. The highest sand value was 74.0%, which occurred at 20 cm. The average sand fraction was 29.1% (Figure 4).

## **DISCUSSION**

### **Definitions of local sand and far travelled dust**

The Fraser Island sand dunes are composed of quartz sand (Boyd, Ruming, Goodwin, Sandstorm, & Schroder-Adams, 2008; Little, 1986). Despite notions that the levels of silicon in the core should correlate to the percentage of sand as defined by grain size, this is not what is observed (Figure 6). Thus, silicon must be being introduced into the core in grain sizes that do not reflect sand as defined by grain size. Sand is usually defined as a function of grain size, with sand being classed as 4 to -1 on the Krumbein  $\Phi$  scale (Pye & Tsoar, 2009). The most reasonable explanation for the lack of relationship between silicon and sand, is that some sand grains have undergone an advanced stage of weathering, before being deposited into the lakes, whilst still keeping the same elemental composition (Little, 1986). Such grains are known as aeolian sandy silts (Pye & Tsoar, 2009). Quartz grains on Fraser Island have been described as falling into four distinct categories based on grain size and morphology

(Little, 1986); clear, un-etched quartz; milky quartz; saccharoidal quartz; and microgranular quartz. The two latter categories are recognised as being highly weathered (Little, 1986). Despite the size and morphological categorisation of the quartz grains, Little et al. (1987) claim that all categories are nearly pure quartz as confirmed by XRD. As the size of sand grains decrease into silt sized quartz, the grains are more likely to be lost from the dunes via saltation (Pye & Tsoar, 2009) resulting in transportation and accumulation in the lake. Thus for the rest of this paper, references to sand will include local quartz of sand dune origin, of 6 to -1 on the Krumbein  $\Phi$  scale, including sand as well as coarse and medium sized silt.

Dust is defined by previous authors as the particle sized fraction that falls between 10 and 6  $\Phi$  on the Krumbein phi scale (Pye & Tsoar, 2009; Reynolds, Frank, & Halliday, 2006). Some studies claim that only clay may contribute to far travelled dust (Petherick et al., 2009), however this paper will consider dust as the former definition, including the fine silt fraction.

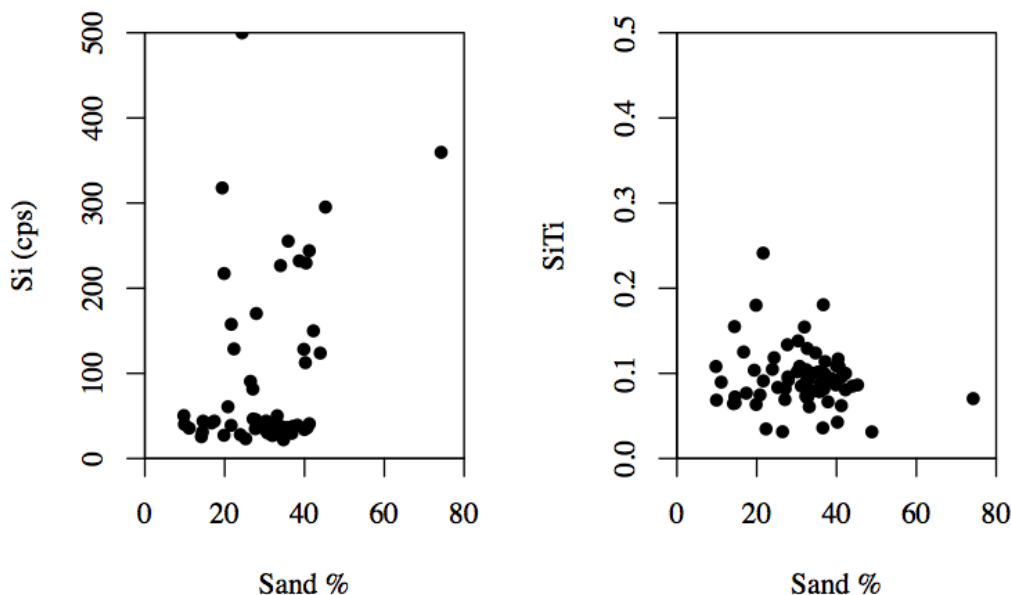


**Figure 6.** Si in cps against sand as considered by grain size, and Si/Ti against sand as considered by grain size.

### **PCA and how elements relate to dust (regional) or sand (local) inputs.**

Considering the principle components analysis (PCA) of the 12 most highly occurring elements, it is clear that Zr, Ti and K are correlated with Si, whilst Ca, Fe and Sr are entirely non correlated to these elements, but have a high correlation to each other. This suggests that the Si, Zr, Ti and K are being introduced by an entirely different source to Ca, Fe and Sr, and these sources have no relationship to each other.

Based on the particle size analysis, and that the quartz sands are locally sourced, it is assumed that the elements correlated to Si (Zr, Ti and K) are being introduced as sand. The relationship between Ca, Fe and Sr, is not correlated to these elements (Ca, Fe and Sr) are not the same processes depositing the sand related elements. For lithics that are not local material to be present in the lake, they must be from an alternate source. Hence, this material is considered the dust component of the core. Since the deposition of dust is a factor of continental scale aridity and wind, and the transport of sand is due to local processes, it is expected that they should be occurring independent to one another.

### **Comparison of discrete and continuous XRF samples**

Extreme differences between the continuous and discrete XRF elemental abundances occur. The continuous record was produced on organic rich sediment, and the discrete samples were inorganic. A potential cause for the differences seen between the XRF analyses is the treatment process that the inorganic sediment was subject to. The digestion process was extreme, and elements such as Ca which were present in high



abundances in the continuous data were absent in the discrete data, potentially as a result of the digestion.

### **Discontinuity of the record**

The sediment record of Basin Lake is discontinuous, with three hiatuses identified in the Basin Lake record. The first and longest hiatus occurs between 49.7-22.9 ka. Two shorter hiatuses occur during the Holocene from approximately 12-11 ka and 8.7-5.1 ka. Other records from Fraser Island also record hiatuses in sedimentation, however these hiatuses occur at different times in sedimentation history. Donders et al. (2006) recorded a hiatus in sedimentation at Lake Allom, from 28 ka to 10 ka, with other authors documenting hiatuses of shorter time periods, and later onsets (Longmore, 1998).

The hiatuses lead to four distinct periods of sedimentation through the core as seen by the iTrax record and levels of inorganic content. Between the periods that are seen, there have been significant shifts in the origin of the source material, and the nature of deposition.

### **Segment A, 404-262 cm, (>49.7 ka)**

The two deepest radiocarbon dates returned ages of 49.7 ka and 50.2 ka, with approximately 1.5 m of sediment separating the materials dated. These dates are close to the age limit of radiocarbon dating, and therefore are not considered of a reliable age. Studies of the reliability of radiocarbon dates have found that the closer to the radiocarbon limit that a date is, the less reliable it is, with suggestions that dates of 35-50 ka should be interpreted with caution (Chapell et al. 1996). Within this range (35-50

ka), the true age of dated material may be substantially older than the date that is returned (Chapell et al. 1996).

For these reasons, the two dates of 49.7 ka and 50.2 ka, are recorded herein as minimum ages. Hence the deepest section of the core is only known as older than 50.2 ka, and cannot be compared to other records. Future studies on this site may include alternative dating methods, in particular optically stimulated luminescence dating, which can date much older sediments. This would allow for the ability to constrain changes in Basin Lake, including sedimentation rates, as well as allowing comparisons to occur across sites.

Throughout segment A the percentage of sand is some of the lowest recorded in the entire core, apart from a large spike in sand influx between 380-365 cm. Levels of Fe increase with increasing Si, indicating Fe is being introduced with sand. Fe also increases when Si levels do not, and at these times is correlated with Ca, indicating Fe is also being introduced to the lake independent to sand. The variability in the minor elements being added to the sediment indicates a non-consistent source of the lithic sediment. The PCA plot (Figure 5) indicates that the elements which, as discussed, are associated with regional scale dust, are dominant throughout this section of the core. This evidence, combined with grain size analysis, indicates that variably sourced dust is accumulating in the lake at this time, consistent with studies from NSI (Petherick 2012). The large variability of the source material indicates that a large region must be experiencing arid conditions to supply the material (Petherick 2012), which is consistent with regional scale aridity.

The small spike in sand influx indicates a locally dry period, as it reflects what is seen later during the LGM. The movement of sand from dunes is believed to be due to

increased windiness and aridity during the LGM (Levin, 2011). The data suggests that this event could be more extreme than the LGM. Longmore and Heinjis (1999) also recorded a period prior to the LGM appearing to be drier than the LGM, which remains consistent with this interpretation.

### **Hiatus I (~28kyr)**

The first hiatus was found when material was dated at 256 cm and 266 cm, returned ages of 18.5 ka and 46 ka, respectively. Thus, approximately 28 kyr occurs within the 10 cm, which is also the location of the extreme change in the iTrax results. The hiatus boundary was identified at 262 cm, based on both the age model and the extremely low moisture contents in the sediment (also used by Donders et al. (2006) to identify hiatuses). Other records reflect hiatuses over the same time period, although of different length (Donders et al., 2006; Longmore, 1998), which has been interpreted as either a dry lake or a seasonally dry lake. Considering the other records show shorter hiatuses, then the length of this hiatus suggests that they may be due to a dry lake, which in Basin Lake, may have also contributed to erosion of the top sediment.

### **Segment B, 262-235 cm (LGM)**

The Last Glacial Maximum was identified in this record as a result of the dated material. The only date within this section was 18.5 ka at 308 cm, with the other dates coming directly before or after inferred hiatuses. Material at 231cm returned a date of 9.5 ka, coupled with the date at 321 cm of 46 ka. Due to having only one date in this section, the rate of sedimentation cannot be derived, only that the segment is within the LGM. Extreme conditions in this segment support the claim that it is different to what is going on above and below it.

High levels of sand were being deposited throughout this section of the core. The amount of sand peaks at 255 cm, drops off and has two local peaks at 240 and 230 cm. High sedimentation accumulation is consistent with records spanning the LGM at nearby North Stradbroke Island, which document peak sediment flux at 21.7 ka (Petherick, McGowan, & Moss, 2008). Whilst the level of sand input has increased substantially, the levels of dust being deposited does not decrease. The higher levels of minor elements in this section of the core than in other sand dominated periods of the core is an indication that there was higher dust input throughout this section. This is based upon the comparison of local quartz sand, and a higher variability in source material, which indicates a foreign source. Whilst other sections with high sand input also contain dust, the amount of dust found in section B, along with it being the most variable in composition, indicates extreme local (Fraser Island) and regional (continental) aridity, consistent with other records (Petherick et al., 2008). This is supported by the PCA of the elemental composition (Figure 5), which suggests that the elements accumulating in the core are associated with local sand.

### **Segment C, 235-68 cm, 11-8 ka**

It is possible that a hiatus may occur between Segment B and Segment C until 11 ka. Due to the lack of sedimentation rate in Segment B such a claim cannot be made, as the location and duration a hiatus cannot be inferred.

For the most of this section of the core, there is very little inorganic material accumulating in the lake. Si is comparatively a less important part of the inorganic deposition in this section, with Ca and Fe being more dominant. Sand inputs from the island are lower during this time period, with dust inputs remaining high.

The accumulation rate for this section of the core is 40 yr/cm. Higher dust inputs in this section of the core are consistent with studies from nearby North Stradbroke Island, which saw the highest levels of dust input at this time (McGowan et al., 2008; Petherick et al., 2009). This is supported by the PCA (Figure 5) which suggests that the dominant source of material accumulating through this section is dust. The composition of the dust does not suggest as variable source material as the previous sections, which indicates that although there may not be extreme, continental scale aridity, there is some regional aridity allowing the transport and deposition of regional dust into the lake.

## **Hiatus II**

A second hiatus occurs at 68 cm, and is identified by the ages of the material dated, and the extreme change in inorganic and moisture content as well as elemental compositions which occur during this period. Material at 50 cm is dated at 3.7 ka, and material at 76 cm is dated at 8ka. The two neighbouring sections are significantly different, with sudden changes occurring. A hiatus at this time is consistent with other records, with Lake Allom (Longmore, 1998) on Fraser Island exhibiting a hiatus from 5.8-6.8 ka (Donders et al., 2006) and Old Lake Coomboo Depression suggesting lower lake conditions from 8.5-2.5 ka (Longmore, 1998).

## **Segment D 0-68 cm, 0-5 ka**

5 ka to present shows the highest amount of inorganic material accumulating in the lake. High levels of Si, Fe and Ti occur. Grain size analysis indicates dominant local sand inputs. Values of Si, Fe, Ca and Ti are coupled, indicating that they are introduced from the same source. This input is dominantly quartz, with included kaolinite and illite (Table 3).

These combinations suggests that the bulk of the sediment input is sand, although some of these changes might be attributed to small inputs of silt and clay, however this fine aeolian material is diluted by the large sand inputs. The accumulation rate in this segment, at 40 years per cm, is a dramatic increase from the previous segment, where sedimentation is only half this. The higher local sediment inputs is consistent with studies on North Stradbroke Island, which claim that percentage of dust that is entering into the sediment at this time is the lowest in their record (Petherick et al., 2009).

High levels of sand input that are seen at the start of this section are not maintained throughout the section, instead dropping rapidly before varying throughout the remainder of the core. Other records of lakes across a more regional scale indicate overall drier conditions throughout this period than at other times in the record (Bowler, 1981). It is suggested that dry periods allow dune transgression, hence why more sand is accumulating during this period (Lees, 2006).

The variability of the record could be explained by alternating wet and dry conditions. Periods of aridity leads to increased local sand inputs, while periodical wet events explains the decreased influxes of localised sand. The past 3 kyr has often been characterised by greater climatic variability and intensification of the ENSO climate phenomenon. The highly variable nature of Basin Lake over the last 3 kyr is indicative of an ENSO dominated climate. An increase in the influence of ENSO after 3 ka at Basin Lake is consistent with other records from Eastern Australia (Donders, Haberle, Hope, Wagner, & Visscher, 2007; Donders et al., 2006; Moy, Seltzer, Rodbell, & Anderson, 2002; Shulmeister & Lees, 1995)

## CONCLUSIONS

This study of Basin Lake addresses knowledge gaps in geochemical records on Fraser Island.

- Prior to 49 ka, regional scale aridity resulted in far-travelled dust becoming the primary source of inorganic material supplied to lake sediments on Fraser Island. The local environment experienced little variability, with little island sand deposited into the lake.
- The LGM was a period of extreme local and regional aridity, resulting in high levels of island sand and far travelled dust depositing into the lake.
- In the period of 11-8ka, there was continued deposition of dust from regional sources, and little deposition of sand from local sources, indicating less variable, calmer condition.
- During the Late Holocene, from 5 ka to present, ENSO has had increased influence on the climate with highly variable conditions resulting in large sediment influxes into the lake.

## **ACKNOWLEDGMENTS**

I would like to thank my exceptional supervisor, Dr. Francesca McInerney, who has supported, encouraged and guided me continuously throughout the entire year. I would like to thank my secondary supervisors, Dr. Jonathan Tyler and Dr. John Tibby, who have both gone above and beyond the role of ‘secondary’ supervisors with the support they have both offered. I would like to thank the Australian Nuclear Science and Technology Organisation, for their support under the ANSTO portal grant 10932 for providing the platform to collect data for this project, in particular I would like to thank Patricia Gadd and Atun Zawadski. I would like to thank the Geological Society of Australia Endowment Fund for their support of this project. I would like to thank Jonathan Marshall, Glenn McGregor and Cameron Schultz from the Queensland Department of Science, Information Technology and Innovation, and Dr. Cameron Barr and Haidee Cadd from the University of Adelaide for the collection of the core this project was based on. I would like to thank Robyn Williamson, Jake Andrea, Haidee Cadd, Georgina Falster for their support. I would also like to thank my fellow honours students, in particular, Julia Short, Thomas Baggs and Mathew Raven.



## REFERENCES

- ATAHAN, P., HEIJNIS, H., LE METAYER, P., GRICE, K., TAFFS, K., HEMBROWN, S., . . . MIX, A. (2013). *Late Quaternary environmental change at Lake McKenzie, in subtropical eastern Australia; evidence from sedimentary carbon, nitrogen and biomarkers*. Paper presented at the Australasian Environmental Isotope Conference, Perth, WA.
- BLAAUW, M., & CHRISTEN, J. A. (2011). Flexible paleoclimate age-depth models using an autoregressive gamma process. *Bayesian Analysis*, 6(3), 457. doi: 10.1214/11-BA618
- BOWLER, J. M. (1981). Australian salt lakes; A palaeohydrologic approach. *Hydrobiologia*, 82(431-444). doi: 0018-8158/81/0823-0431
- BOYD, R., RUMING, K., GOODWIN, I., SANDSTORM, M., & SCHRODER-ADAMS, C. (2008). Highstand transport of coastal sand to the deep ocean: A case study from Fraser Island, southeast Australia. *Geological Society of America*, 36(1), 15-18. doi: doi.org/10.1130/G24211A.1
- DONDERS, T. H., HABERLE, S. G., HOPE, G., WAGNER, F., & VISSCHER, H. (2007). Pollen evidence for the transition of the Eastern Australian climate system from the post-glacial to the present-day ENSO mode. *Quaternary Science Reviews*, 26(11-12), 1621-1637. doi: 10.1016/j.quascirev.2006.11.018
- DONDERS, T. H., WAGNER, F., & VISSCHER, H. (2006). Late Pleistocene and Holocene subtropical vegetation dynamics recorded in perched lake deposits on Fraser Island, Queensland, Australia. *Palaeogeography, Palaeoclimatology, Palaeoecology*, 241(3-4), 417-439. doi: 10.1016/j.palaeo.2006.04.008
- FRAUEN, C., & DOMMENGET, D. (2010). El Nino and La Nina amplitude asymmetry caused by atmospheric feedbacks. *Geophysical Research Letters*, 37(18), 1-6. doi: 10.1029/2010GL044444
- GONTZ, A. M., MOSS, P. T., C.R., S., PETHERICK, L., MCCALLUM, A., & SHAPLAND, F. (2015). Understanding past climate variation and environmental change for the future of an iconic landscape - K'gari Fraser Island, Queensland, Australia. *Australasian Journal of Environmental Management*, 22(2), 105-123. doi: 10.1080/14486563.2014.1002120
- HEMBROW, S., & TAFFS, K. (2012). Water quality changes in Lake McKenzie, Fraser Island, Australia; a palaeolimnological approach. *Australian Geographer*, 43(3), 291-302.
- LEES, B. (2006). Timing and formation of Coastal Dunes in Northern and Eastern Australia. *Journal of Coastal Research*, 22(1), 78-89. doi: 10.2112/05A-0007.1
- LEVIN, N. (2011). Climate-driven changes in tropical cyclone intensity shape dune activity on Earth's largest sand island. *Geomorphology*, 125, 239-252. doi: 10.1016/j.geomorph.2010.09.021
- LITTLE, I. P. (1986). Mobile iron, aluminium and carbon in sandy coastal podzols of Fraser Island, Australia: a quantitative analysis. *Journal of Soil Science*, 37, 439-454.
- LONGMORE, M. E. (1998). The Mid-Holocene 'dry' anomaly on the mid-Eastern coast of Australia: Calibration of palaeowater depth as a surrogate for effective

- precipitation using sedimentary loss on ignition in the perched lake sediments of Fraser Island, Queensland. *Palaeoclimate: Data and modelling*.
- LONGMORE, M. E., HEIJNIS, H., PARTRIDGE, T. C., KERSHAW, A. P., & IRIONDO, M. H. (1999). Aridity in Australia; Pleistocene records of palaeohydrological and palaeoecological change from the perched lake sediments of Fraser Island, Queensland, Australia. *Quaternary International*, 57, 35-47. doi: 10.1016/S1040-6182(98)00048-2
- MARSHALL, S. K., FONTAINE, K., KILGOUR, P. L., & LEWIS, S. L. (2015). Regional Hydrogeology Characterisation of the Maryborough Basin, Queensland: Technical report for the National Collaboration Framework Regional Hydrology Project. In C. J. Pigram (Ed.), *Record 2015/14* (pp. 1-117): Geoscience Australia, Canberra.
- MARTIN-REY, M., RODRIGUEZ-BONSECA, B., & POLO, I. (2015). Atlantic opportunities for ENSO prediction. *Geophysical Research Letters*, 42(16), 6802-6810. doi: 10.1002/2015GL065062
- MARX, S. K., MCGOWAN, H., & KAMBER, B. S. (2009). Long-range dust transport from eastern Australia; a proxy for Holocene aridity and ENSO-type climate variability.
- MCGOWAN, H., PETHERICK, L., & KAMBER, B. S. (2008). Aeolian sedimentation and climate variability during the late Quaternary in southeast Queensland, Australia. *Palaeogeography, Palaeoclimatology, Palaeoecology*, 265(3-4), 171-181. doi: 10.1016/j.palaeo.2008.05.011
- MOY, C., SELTZER, G., RODBELL, D., & ANDERSON, D. (2002). Variability of El Nino/Southern Oscillation activity at millennial timescales during the Holocene epoch. *Nature*, 420, 162-165. doi: 10.1038/nature01194
- NIETO-MORENO, V., MARTINEX-RUIZ, R., GALLAGO-TORRES, D., GIRALT, S., GARCIA-ORELLANA, J., MASQUE, P., . . . ORTEGA-HUERTAS, M. (2014). Palaeoclimate and palaeoceanographic conditions in the westernmost Mediterranean over the last millennium: an integrated organic and inorganic approach. *The Geological Society of London*, 172(2). doi: doi.org/10.1144/jps2013-105
- PETHERICK, MCGOWAN, H., & MOSS, P. (2008). Climate variability during the last glacial maximum in eastern Australia; evidence of two stadials? *Journal of Quaternary Science*, 23(8), 787-802. doi: 10.1002/jqs.1186
- PETHERICK, MCGOWAN, H. A., KAMBER, B. S., BAUER, B. O., & LANCASTER, N. (2009). Reconstructing transport pathways for late Quaternary dust from eastern Australia using the composition of trace elements of long traveled dusts. *Geomorphology*, 105((1-2)), 67-79. doi: 10.1016/j.geomorph.2007.12.015
- PYE, K., & TSOAR, H. (2009). *Aeolian Sands and Sand Dunes*. Leipzig, Germany: Springer-Verlag Berlin Heidelberg.
- REYNOLDS, B. C., FRANK, M., & HALLIDAY, A. N. (2006). Silicon isotope fractionation during nutrient utilization in the North Pacific. *Earth and Planetary Science Letters*, 244, 431-443. doi:
- ROBINSON, M., & DOWSETT, H. (2012). *Why Study Palaeoclimate* (Vol. 2010-3021, pp. 1-2): U.S. Geological Survey.

- SHULMEISTER, J., & LEES, B. (1995). Pollen evidence from tropical Australia for the onset of an ENSO-dominated climate at c. 4000BP. *The Holocene*, 5(1), 10-18.
- TEKAN-KELLA, M. S., CHITTLEBOROUGH, D. J., FITZPATRICK, R. W., THOMPSON, C. H., PRESCOT, J. R., & HUTTON, J. T. (1990). Thermoluminescence Dating of Coastal Sand Dunes at Cooloola and North Stradbroke Island, Australia. *Australian Journal of Soil Research*, 28, 465-481.
- THOMAS, M. F., NOTT, J., MURRAY, A. S., & PRICE, D. M. (2007). Fluvial response to late Quaternary climate change in NE Queensland, Australia. *Palaeogeography, Palaeoclimatology, Palaeoecology*, 251(1), 119-136. doi: 10.1016/j.palaeo.2007.02.021
- WOLTERING, M., ATAHAN, P., GRICE, K., HEIJNIS, H., TAFFS, K., & DODSON, J. (2014). Glacial and Holocene terrestrial temperature variability in subtropical east Australia as inferred from branched GDGT distributions in a sediment core from Lake McKenzie. *Quaternary Research*, 82(1), 132-145.

## **APPENDIX A: EXTENDED METHODS**

Sediments were cored from Basin Lake, Fraser Island, using a Bolivia Corer.

### **Core splitting**

A vibro saw was used to cut into the PVC tubing without cutting all the way into the PVC, and a Stanley knife was used to finish the final cut into the PVC tubing. A fishing wire was placed between the cuts on the pipe and ran the length of the pipe. Duct tape was placed on one side of the pipe holding the join together on one side. Using a spatula knife between the two halves of sediment, the two halves were cautiously separated. Using a spatula knife again, the very top layer of sediment was removed to avoid contamination, as well as any visible PVC removed. The duct tape holding the two halves together was removed. The core was wrapped in Glad Wrap, ensuring that all of the exposed sediment was in contact with the glad wrap and there were no air bubbles. Three layers of Glad Wrap were used and Duct tape was used after the last layer on the ends to ensure it wouldn't unwrap. The core was refrigerated horizontally.

### **Loss on ignition**

Dry 10mL crucibles were weighed and the weight recorded. Approximately ½ cubic centimeter of sediment was weighed into the dried crucibles at centimeter intervals and the weight recorded. The wet sediment was dried in an oven at 105°C for at least 12 hours. The dry samples were then weighed, and placed in a muffle furnace that ramped to 550°C. Once the furnace had reached 550°C the samples were timed for 4 hours. The furnace was left overnight to cool, and the samples were removed and weighed. This method of organic matter analysis was chosen due to cost effectiveness and rapid analysis.

### **ITRAX**

The core was taken to ANSTO at Sydney for iTrax XRF analysis. The top layer of the sediment was scraped, and a 1nm thick film placed over the surface of the sediment to protect it from the laser. The data resolution was selected at 1mm. A chromium-helium target x-ray tube was used. The XRF conditions were 30kV 55mA and the x-radiograph conditions were 50 kV 30 mA. 10second count time/increment was used. This method of chemical analysis was chosen due to the high resolution of data that may be produced in a rapid period of time, and relative cost effectiveness.

## **Particle size analysis**

For particle size analysis, the organic matter must first be removed from the sediment, so that the particle size distribution results in only the particle size of inorganic matter. The following method was adapted from a method described in the United States Soil Survey Methods Manual, and was chosen due to the ability of the method to remove high levels of organic matter without destroying the inorganic matter.

10 g of sediment was sub sampled from and measured into a 50 mL centrifuge tube. 10 mL of RO water is added at room temperature as well as 1mL of hydrogen peroxide (50%). The samples are placed in a water bath and heated to 80°C. An additional 1mL of hydrogen peroxide is added. After 10 minutes 2 mL increments of hydrogen peroxide (50%) is added to the sample every 5-10 minutes, up to 10 mL. After the final increment of hydrogen peroxide is added the samples remain in the water bath so that their total time in the water bath is 3 hours, to allow any unreacted solution to complete the reaction. The samples were centrifuged at 4000 rpm for 25 minutes, and the liquid decanted. The process was repeated five times for each sample, to ensure that all of the organic matter was removed. Once the organic matter was entirely removed, 1 mL of sodium hexametaphosphate (0.5 M) was added and the samples were ultrasonicated for 15 minutes.

The particle size analysis was undertaken on a Mastersizer 2000. This method of particle size analysis is used due to the cost effectiveness for running samples, as well as the high resolution and rapid analysis times in comparison to alternative methods. The samples were placed in 50 mL beakers and magnetically stirred. The sample was transferred into the sample jar as individual aliquots, until the obscuration level was between 10% and 20%, ideally 15%. The sample was then ultrasonicated for 20 seconds. At the completion of the ultrasonication the measurement began. At the completion of each measurement, two beakers of clean tap water was run through the sampler for at least 1 minute each to rid the sampler of any of the previous sample.

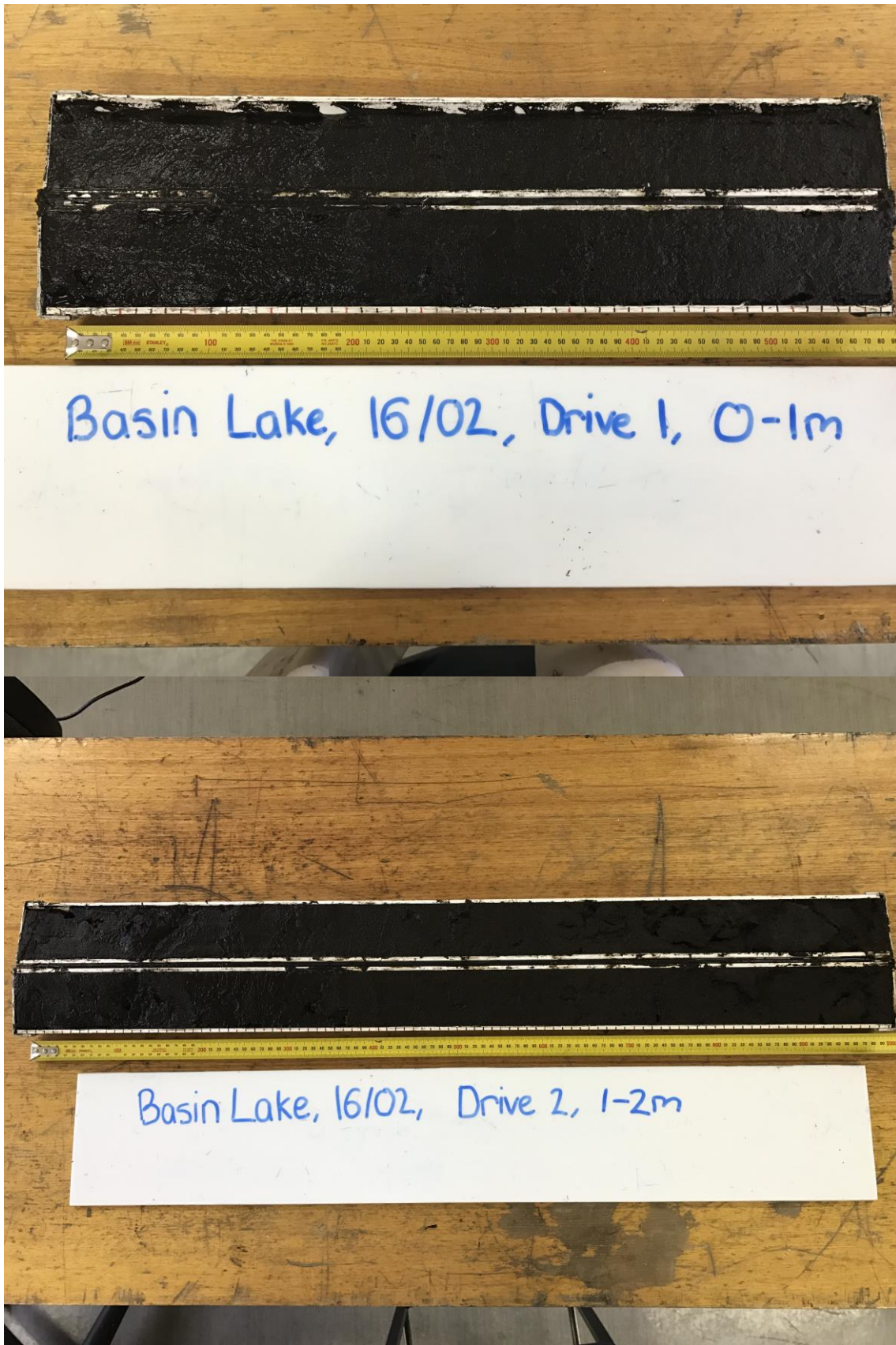
## **XRD**

Twenty samples through the length of the core were selected for XRD analysis. They were prepared using hydrogen peroxide in the method described for particle size analysis. The samples were scanned for XRD at the University of Adelaide.

## **XRF**

Due to the semi-quantitative nature of the ITRAX analysis, XRF was chosen due to its quantitative nature as a method of calibrating the ITRAX data. The XRF was due to be performed on the same samples as the XRD analysis, unfortunately, 20 samples were required to produce a calibration, and only 5 samples were of sufficient sample size to be analysed. The samples were ground with a mortar and pestle so that 85% of the sample passes through 75nm. The samples were then sent to Bureau Veritas to undergo traditional XRF analysis.

**APPENDIX B: CORE PHOTOGRAPHS**





Basin Lake, 16/02, Drive 3, 2-3m



Basin Lake, 16/02, Drive 4, 3-4m

